ChemBioChem

Combining Chemistry and Biology

Chemistry Europe

European Chemical Societies Publishing

Accepted Article

Title: Development of Gene-Targeted Polypyridyl Triplex Forming Oligonucleotide Hybrids

Authors: Nicoló Fantoni, Bríonna McGorman, Zara Molphy, Daniel Singleton, Sarah Walsh, Afaf H. El-Sagheer, Vickie McKee, Tom Brown, and Andrew Kellett

To be cited as: *ChemBioChem* 10.1002/cbic.202000408

Link to VoR: https://doi.org/10.1002/cbic.202000408

WILEY-VCH

WILEY-VCH

FULL PAPER

Development of Gene-Targeted Polypyridyl Triplex Forming Oligonucleotide Hybrids

Nicolò Zuin Fantoni,[1†] Bríonna McGorman,[1‡] Zara Molphy,[1,2‡] Daniel Singleton,[3] Sarah Walsh,[4,5] Afaf H. El-Sagheer,[4,6] Vickie McKee,[1,7] Tom Brown,[4] & Andrew Kellett*[1,2]

Abstract: In the field of nucleic acid therapy there is major interest in the development of libraries of DNA-reactive small molecules which are tethered to vectors that recognize and bind specific genes. This approach mimics enzymatic gene-editors, such as ZFNs, TALENs and CRISPR-Cas, but overcomes limitations imposed by the delivery of a large protein endonuclease which is required for DNA cleavage. Here, we introduce a chemistry-based DNA cleavage system comprising an artificial metallo-nuclease (AMN) that oxidatively cuts DNA, and a triplex forming oligonucleotide (TFO) that sequence-specifically recognises duplex DNA. The AMN-TFO hybrids coordinate Cu(II) ions to form chimeric catalytic complexes that are programmable—based on the TFO sequence employed—to bind and cut specific DNA sequences. Use of the alkyne-azide cycloaddition 'click' reaction allows scalable and high-throughput generation of hybrid libraries that can be tuned for specific reactivity and gene-of-interest knockout. As a first approach, we demonstrate targeted cleavage of purine-rich sequences, optimisation of the hybrid system to enhance stability, and discrimination between target and *off*-target sequences. Our results highlight the potential of this approach where the cutting unit, which mimics the endonuclease cleavage machinery, is directly bound to a TFO guide by click chemistry.

Introduction

Recently, there have been remarkable advances in therapies that target nucleic acids. For example, the sequence-specific recognition of RNA is central to antisense oligonucleotide (ASO) technologies, where short interfering RNA (siRNA) and ASOs target mRNA and become cleavage substrates for Argonaute or RNase H, respectively.[1,2] Although intervention at the mRNA level is an effective therapeutic approach, it does not alter the underlying genetic code and hence gene silencing remains transient. Antigene technologies, however, provide a potential means to permanently alter the mammalian genome.[3] Here, genetic modifications are caused by directed epigenetic mutations, which affect nucleobase sequence integrity (*e.g.* strand insertions, single-point mutations),[4,5] or by code disruptors (*e.g.* deletions, alkylation, oxidative damage).[6,7] The advantage of antigene technologies therefore lies in their capacity to target and permanently modify disease-specific genes.

Artificial metallo-nucleases (AMNs) provide an alternative cleavage strategy to ASOs and state-of-art gene editing systems. They rely on redox metals to generate reactive oxygen species (ROS) that damage nucleotides to initiate strand excision and gene silencing.[8,9] AMNs are characterised by both the metal ion present and the shape and charge of the DNA-coordinating ligand. Copper-based AMNs are attractive due to their versatile coordination environments, oxygen activation mechanisms, intrinsic bioavailability and their tolerance in biological systems.[10] The first discovered AMN $[Cu(1,10\text{-phenanthroline})_2]^{2+}$ (Cu-Phen) was shown to semi-intercalate and oxidise DNA from the minor groove in the presence of a reductant (*e.g.* ascorbate).[7,11] More recently, polypyridyl and macrocyclic copper-binding AMN architectures have been identified.[12–16] Copper AMNs have so far been used in DNA footprinting,[7] recombinant protein production,[17] chemotherapy,[18] and for nucleobase discrimination.[19]

Efforts to engineer site-specific nucleases have focused on tethering the AMN to sequence-directing groups such as DNA-binding proteins, polyamides, and polynucleotides.[11,20–27] Early work on directed systems showed sequence-specific cleavage could be achieved when Fe-EDTA or Cu-Phen complexes were covalently modified with distamycin derivatives.[20,28,29] However, the laborious design and preparation of polyamides diverted research toward TFOs as a more efficient targeting vector. TFOs can be programmed to specifically recognise long DNA regions and their nucleobase recognition relies on Hoogsteen base pairing, thereby providing ease-of-design compared to polyamides. Using this strategy, targeted DNA cleavage was reported for Fe-EDTA and Cu-Phen conjugates in the presence of exogenous reductant (Figure 1a). Inspired by these first efforts, the discovery of chimeric iron(II),[30,31] cerium(IV),[32] zirconium(IV),[33] rhenium(I),[34] technetium(I),[35] platinum(II)[36] and rhodium(II)[37] DNA recognition systems were later reported. Despite the early success of Fe-EDTA and Cu-Phen hybrids, in these early days of nucleic acid (NA) chemistry the development of hybrids was limited by: (a) complex preparative methods required to produce modified oligonucleotide (ON) building

[1] Dr. Nicoló Fantoni, Ms. Bríonna McGorman, Dr. Zara Molphy, Prof. Vickie McKee and Prof. Andrew Kellett. School of Chemical Sciences and National Institute for Cellular Biotechnology, Dublin City University, Glasnevin, Dublin 9, Ireland. E-mail: andrew.kellett@dcu.ie
[2] Synthesis and Solid-State Pharmaceutical Centre, School of Chemical Sciences, Dublin City University, Dublin 9, Ireland.
[3] Dr. Daniel Singleton. ATDBio Ltd., School of Chemistry, University of Southampton, Southampton, SO17 1BJ, United Kingdom.
[4] Dr. Sarah Walsh, Dr. Afaf H. El-Sagheer and Prof. Tom Brown. Chemistry Research Laboratory, University of Oxford, 12 Mansfield Road, Oxford OX1 3TA, United Kingdom.
[5] ATDBio Ltd., Magdalen Centre, Oxford Science Park, Oxford, OX4 4GA, United Kingdom.
[6] Chemistry Branch, Department of Science and Mathematics, Faculty of Petroleum and Mining Engineering, Suez University, Suez 43721, Egypt.
[7] Department of Physics, Chemistry and Pharmacy, University of Southern Denmark, Campusvej 55, 5230 Odense M, Denmark.
Supporting information for this article is given via a link at the end of the document.

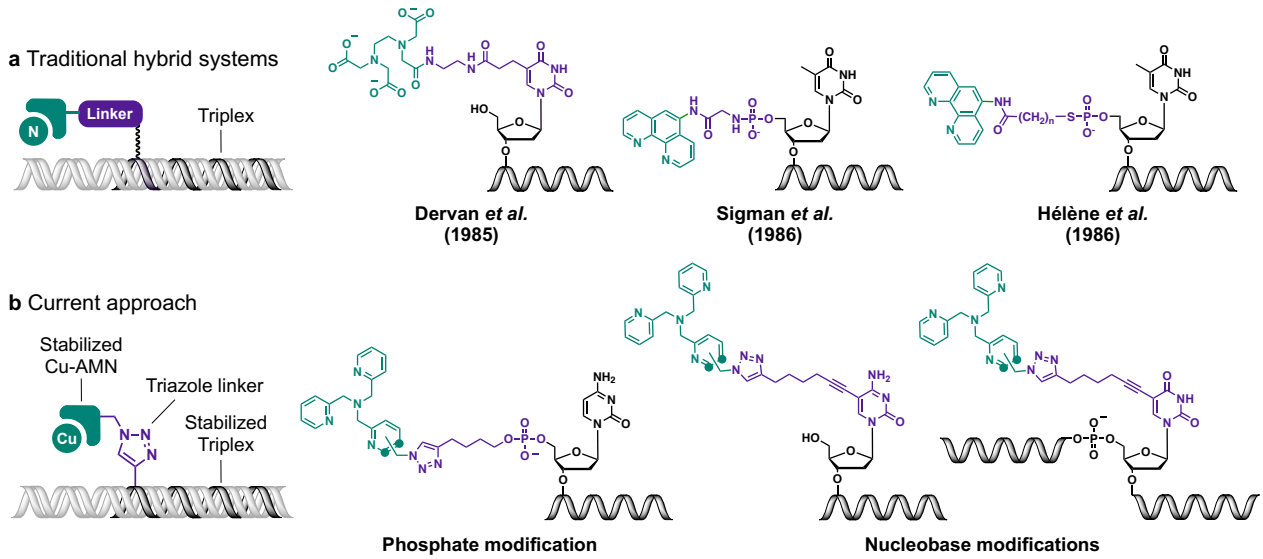

Figure 1. a Molecular structure of the traditional targeted-AMNs where a triplex forming oligonucleotide (dark grey) has been coupled to either EDTA or Phen (green) through peptide linkers (purple). **b** molecular structure of the current synthetic approach via 'click' chemistry and triazole formation to allow high-throughput generation of TFO hybrids with AMN modification either on the phosphate or nucleobase.

blocks[31,38–40] (**Figure 1a**); (b) low stability associated with metal ion dissociation[14]; (c) non-selective (*off*-target) cleavage effects and the need for undesirably high hybrid concentrations required to achieve appropriate binding and cleavage effects[24,40,41]; and (d) the requirement of an adjuvant (*e.g.* spermine) and reductant to stabilise and cleave DNA triplexes, respectively.

Here, we present a new strategy for the generation of TFOs loaded with copper AMNs for targeted oxidative DNA damage. The hybrids are generated by coupling an azide-functionalised AMN with an alkyne-modified TFO using the copper catalysed azide-alkyne cycloaddition (CuAAC) 'click' reaction. Significantly, click chemistry has been identified as a successful strategy to label oligonucleotides with rhenium,[34] platinum[36] and clip-Phen[25] complexes, the latter of which was recently targeted to the Env gene in the HIV-1 genome. Our approach facilitates scalable and high-throughput production of hybrid libraries (**Figure 1b**) with the triazole linkage providing enhanced biological stability compared to previously employed amide linkers. To address limitations associated with copper complex stability, we designed two modified polypyridyl ligands to strongly ligate copper ions. TFOs were targeted to purine-rich regions of the green fluorescent protein (GFP) gene and the cleavage effects of copper-bound hybrids were studied using polyacrylamide gel electrophoresis (PAGE) and quantitative polymerase chain reaction (qPCR). Oxidative cleavage was further investigated using a large GFP cloning vector (6389 bp) and the ROS-mediated cleavage mechanism was probed using a variety of free radical and spin trapping agents. Finally, we demonstrate how engineering the TFO strand with strain-promoted alkyne substituents and thiazole orange (TO) intercalators can provide enhanced triplex stabilisation and DNA cleavage. These efforts may now guide further development of this class of sequence-specific DNA cleaving agents for cellular gene-knockout applications.

Results and Discussion

Design of azide-modified copper-binding scaffolds

We developed synthetic routes to introduce an azide-modification at two different positions of the copper binding polypyridyl ligand TPMA (*tris*-(2-picolyl)amine) (**Figure 2a** and **2b**). Both strategies were designed to maintain (where possible): (a) the use of canonical 'click' reaction conditions to preserve modularity, insensitivity toward oxygen and water, regiospecificity and stereospecificity; (b) green chemistry criteria through the employment of safer solvents, chemicals and easily removable catalysts or reactants; and (c) potential future industrial scalability. In **Route A**, an asymmetric pyridine (**3a**) was prepared from 2,5-pyridinedicarboxylic acid using regioselective functional group conversions. The use of SeO_2 to prepare **3a** allows for regiospecific oxidation of the 2-hydroxyl group due to interaction between the selenium atom and the proximal pyridine nitrogen atom. Schiff-base condensation of **3a** with picolylamine, followed by nucleophilic substitution of **4a** on 2-picolylchloride afforded 5OH-TPMA (**5a**), which was then used as a substrate to release the $5N_3$-TPMA target (**7a**). In **Route B**, 2,6-*bis*-(chloromethyl)pyridine was treated with DPA to form the tripodal scaffold, **1b**. Nucleophilic substitution of NaN_3 on **1b** then afforded $6N_3$-TPMA (**2b**). The isolated copper-binding ligands $5N_3$-TPMA (**7a**) and $6N_3$-TPMA (**2b**) were characterised by ^{1}H-, ^{13}C- and 2D-NMR (**supplementary S-1**) and ESI-MS. Our motivation for developing the $5N_3$-TPMA ligand stemmed from single X-ray analysis of the $[Cu(6N_3\text{-TPMA})(NO_3)](NO_3)\cdot\frac{1}{2}CH_3CN$ complex (**Figure 2c** and **supplementary S-2**). The asymmetric unit (**Figure S-31**) contains two similar but independent $[Cu(6N_3\text{-TPMA})(NO_3)]^+$ cations (**Figure S-32**). These are approximately square pyramidal with a long apical bond to the pyridines carrying the azide group. There is an additional very long bond to a second oxygen donor of the coordinated nitrate ion. Comparison with the structure of $[Cu(TPMA)(Phen)]^{2+}$ (**Figure 2d**) suggests the

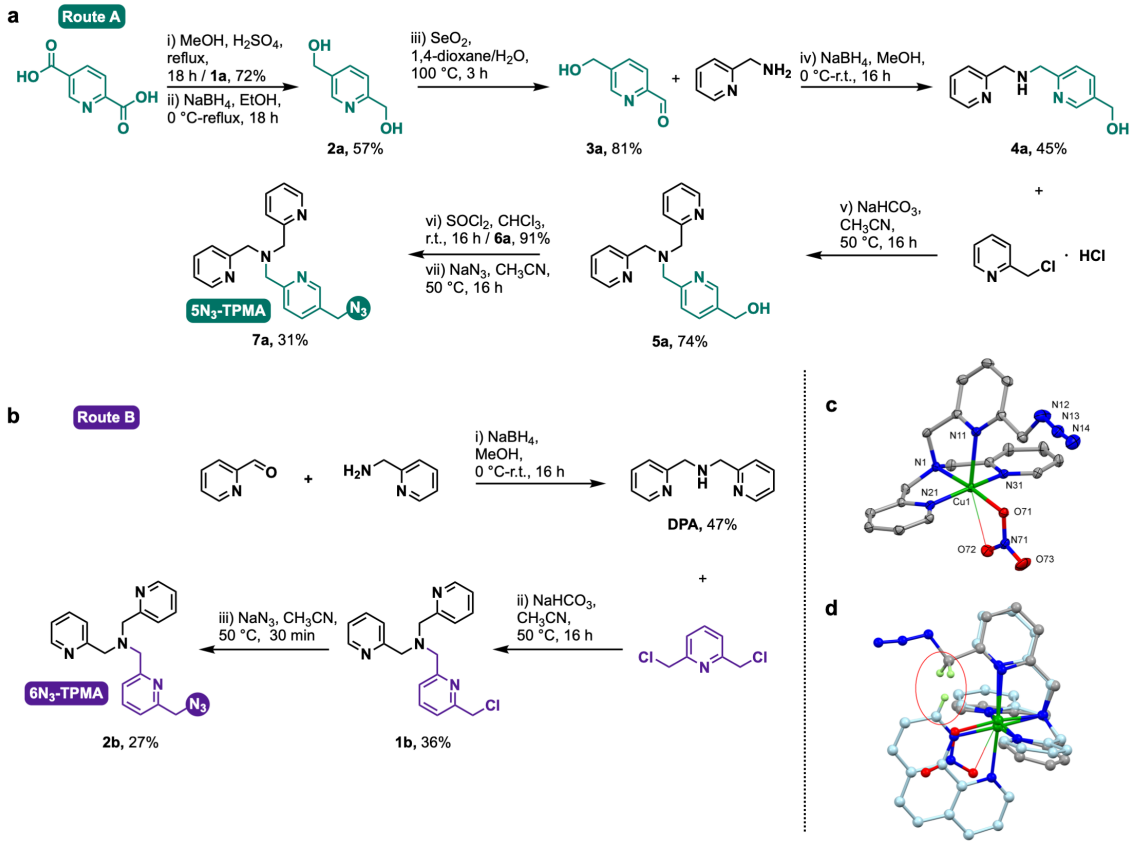

Figure 2. Preparation of AMN ligands: **a** *N*-5-(azidomethyl)pyridine-*N*-di-(2-picolyl)amine ($5N_3$-TPMA, route a, 7a) and **b** *N*-6-(azidomethyl)pyridine-*N*-di-(2-picolyl)amine ($6N_3$-TPMA, route b, 2b); **c** One of the two independent $[Cu(6N_3\text{-TPMA})(NO_3)]^+$ cations showing 50% probability ellipsoids (hydrogen atoms omitted for clarity, long interaction shown as a thin line); **d** Overlay of $[Cu(6N_3\text{-TPMA})(NO_3)]^+$ (carbons shown grey) and $[Cu(TPMA)(phen)]^{2+}$ (carbons shown pale blue; *cf.* **Figure S-34** for structural formulae). Potential interactions between phen and $6N_3$-TPMA hydrogen atoms highlighted (remaining hydrogen atoms omitted for clarity).

methylene carbon in $6N_3$-TPMA prevents accessibility of an additional phenanthrene ligand (or, at least, that the apical pyridine and Phen cannot both bind) due to interaction of the methylene hydrogen atoms with those of the phenanthrene. The azide in $5N_3$-TPMA is remote by comparison reducing the potential for steric hindrance around the metal when clicked to the alkyne-TFO.

Engineering Cu(II)-TFO hybrids with click chemistry

Several factors were taken into account in the design of parallel TFOs: an oligopyrimidine strand was chosen for Hoogsteen base recognition of the target; a recognition site with a low number of consecutive C^+-GC triplets since they are stable only at low pH;[3,42,43] and a minimum number of triplet inversions (*e.g.* G-TA) since they are destabilising.[44] More complex approaches have been developed to circumvent these sequence and pH limitations on triplex stability, but they were not required in this study.[45] We prepared Cu(II)-TFO hybrids (*cf.* **Figure 1b**) by clicking[46] the azide-modified $5N_3$-TPMA and $6N_3$-TPMA, ligands to alkyne-modified oligonucleotides. Click reactions were performed in an anaerobic environment to prevent oxygen activation by the copper catalyst and possible oxidation of the oligonucleotide probe. Three alkyne TFO variations were considered—5′-phosphate-, terminal base-, and internally base-modified sequences. 5′-hexynyl-dN (Mod A), 5′-(5)octadiynyl-dC (Mod B), or internal octadiynyl-dU (Mod C) (**Figure 3a**) TFOs were then clicked by CuAAC to the AMN ligands (*cf.* **Figure 2a & b**). The final library of AMN-TFOs ranged between 16 – 32 nt in length (TFO 1-5; **Figure 3b**). Triplexes contained either one (TFO1) or two (TFOs 2, 4, and 5) G-TA inversions when bound to their target, while TFO3 was fully complementary. The flexible 5′-phosphate modification (Mod A) was designed to target both the major and minor groove of DNA, while Mod B and C target only the major groove. The full alkyne-TFO and AMN-TFO library is presented in **Table S-3 & S-4**.

Triplex formation by AMN-TFO hybrids

Thermal melting experiments were conducted with duplex sequences from the GFP plasmid containing 10 flanking base pairs on each side of the TFO binding site (**Figure 3b**). Studies were carried out under physiological conditions (10 mM PO_4^{3-}, 150 mM NaCl, 2 mM $MgCl_2$) at pH 6.0 to ensure cytosine protonation (**Table S-5** and **Figure S-36**). Alkyne-modified TFOs were first examined for their ability to form triplexes (**Table S-5**).

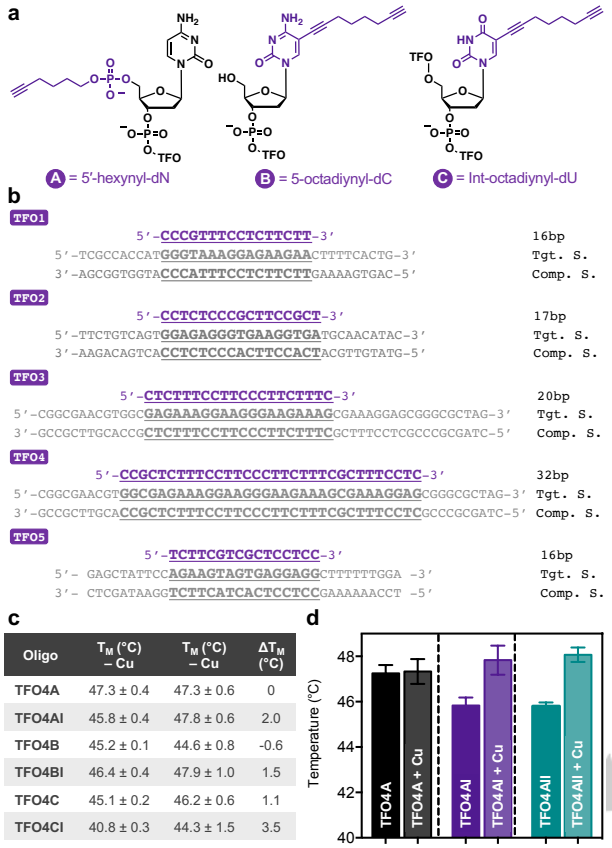

Figure 3. a Alkyne modified nucleotides. **b** TFO sequences (purple) targeting specific regions of a GFP cloning vector (grey). **c** TM of TFO4A hybrids modified with either 6N3-TPMA (I) in the absence or presence of 1 eq Cu(II). d ΔTM of TFO4A hybrids containing alkyne modification clicked to 6N3-TPMA (I) in the absence or presence of 1 eq Cu(II).

Although G-TA inversions are the most stable of the X-TA inverted triplex combination (where X = A, C, G, or T),[44] the presence of two inverted triplets in TFO2 (16 nt) and TFO5 (17 nt) resulted in triplexes that were not stable above 12 °C and thus were not further investigated. TFO1, a 16 nt sequence containing a single G-TA inversion, formed stable triplexes with melting temperatures (T_M) in the range of 19.3 - 24.6 °C depending on the AMN 'click' modification introduced. TFO3A, a 20 nt sequence with no inversion sites, had a T_M value of ~45 °C while TFO4 (32 nt)—containing two inverted triplets—also formed stable triplexes with melting temperatures of ~45 °C or above. Upon conjugating AMNs to TFO sequences, a slight lowering of triplex stability was identified with exception of terminal base modified AMNs (Mod B) (**Figure 3c** and **Table S-5**). These effects may be attributed to steric hindrance exerted by the bulky polypyridyl ligands at the 5′-phosphate termini, while base stacking interactions by the ligands are feasible when positioned at the terminal nucleobase. Coordination of a Cu(II) ion introduced in the form of $Cu(ClO_4)_2$ to AMN-TFO hybrids enhanced triplex stability up to 6 °C (**Figure 3d** and **Table S-5**). As expected, this effect was not observed in the absence of a copper-binding AMN (*i.e.* alkyne-TFOs). Therefore, enhanced stability is likely due to a combination of charge neutralisation and Cu(II)-phosphate binding of the target duplex by the metal-bound AMN—an effect recently identified in a major groove binding copper(II) polypyridyl complex.[47] Although a range of organic modifications for augmenting triplex stability have been reported,[48] to our knowledge this is the first evidence of triplex stabilisation induced by a metal binding adduct.

Targeted oxidative cleavage by AMN-TFO hybrids

We initially assessed triplex formation and oxidative cleavage by Cu(II)-TFO hybrids against a 52 bp sequence from a plasmid containing the GFP gene using polyacrylamide gel

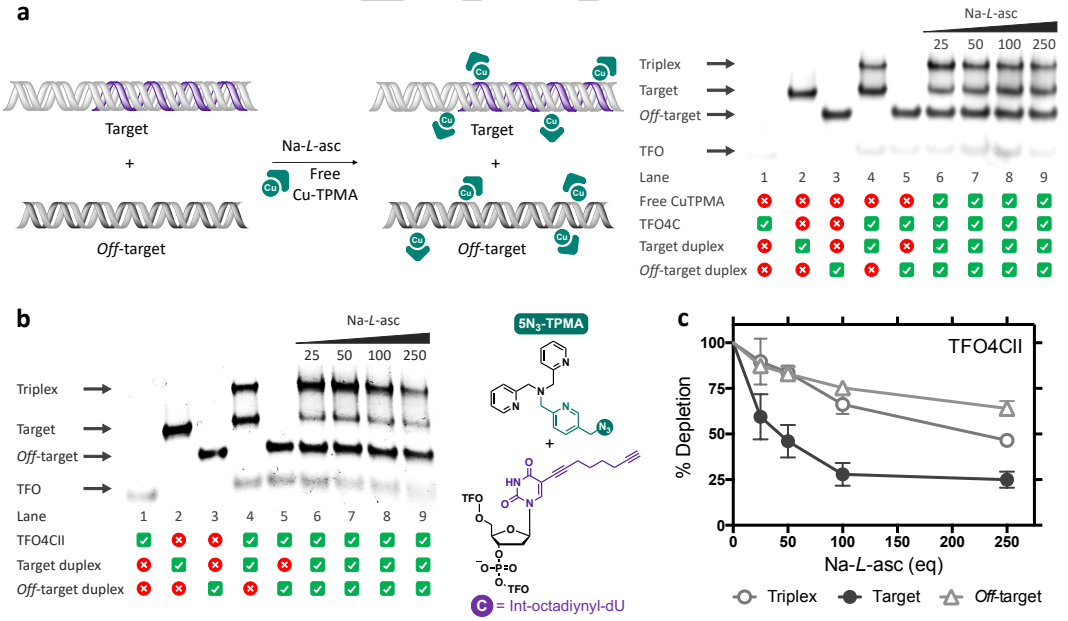

Figure 4. a Cartoon of target and *off*-target duplex treated with free AMN (left), duplex target and off-target (1.25 pmol) treated with a 25 eq mixture of free Cu-TPMA and TFO4C (Cu-TPMA/TFO4C; 1:1) in the presence of increasing concentrations of Na-*L*-asc (25-250 eq to Cu-TPMA/TFO4C; lanes 6-9, right). **b** 25 eq. of Cu(II) bound hybrid TFO4CII was exposed to the target and an *off*-target duplex (1.25 pmol) in the presence of increasing concentrations of Na-*L*-asc (25-250 eq). **c** Densitometry analysis showing target discrimination and cleavage (right).

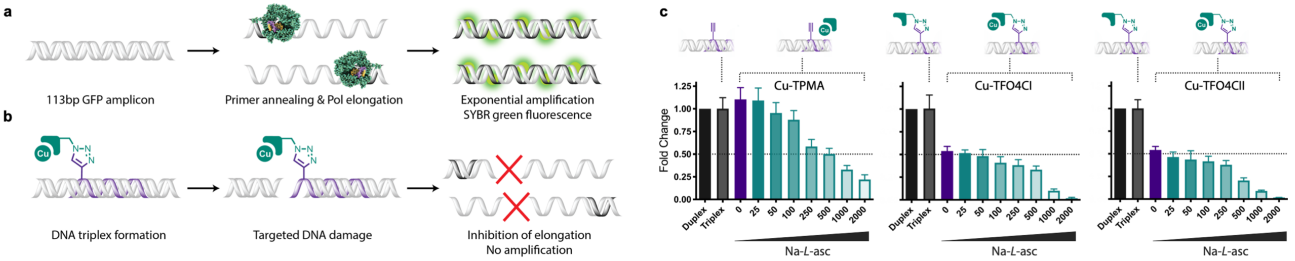

Figure 5. a Illustration of steps involved in a successful qPCR cycle using *Taq* polymerase, primers and SYBR green I; **b** Inhibition of DNA amplification due to oxidative DNA damage of the template strand by the AMN-TFO hybrid; and **c** Target duplex (0.625 pmol) treated with 25 eq. of non-clicked Cu(II)-TPMA complex TFO4CI and TFO4CII in the presence of increasing concentrations of Na-*L*-asc (0-2000 eq. to TFO4C derivative). Resulting DNA damage was analysed by qPCR where the change in threshold cycle between the target (6 h) and control sample (0 h) (target C_T – control C_T) was calculated (ΔC_T). ΔC_T was plotted as linear values ($2^{-\Delta CT}$).

electrophoresis (PAGE) (*cf*. **Figure S-37**). Our studies focused on TFO3 and TFO4 since they formed stable triplexes above 37 °C. Alkyne-modified TFO4A (*i.e*. the probe without clicked AMN) in the presence of Cu(II) and increasing ascorbate produced no cleavage effects towards either the target or *off*-target duplex present *in-situ* (**Figure S-38**). Oxidative damage of the target sequence was also monitored in the presence of the non-clicked Cu(II)-TPMA complex, alkyne-TFO, an *off*-target sequence, and increasing equivalents of reductant (**Figure 4a**). This mixture was not efficient at depleting the target with similar degradation effects observed on the *off*-target. Identical experiments with Cu(II)-bound AMN-TFO hybrids demonstrated targeted cleavage and excellent sequence discrimination at low reductant loading (**Figure S-39**). The presence of an internally clicked AMN results in significant depletion (*cf*. TFO4CII **Figure 4b**) with the target being degraded faster than the *off*-target sequence (72% versus 24% knockdown with 100 eq. Na-*L*-asc, respectively, **Figure 4c**). The decreased intensity in the target duplex band (Figure 4b, Lane 6-9) can be attributed to the cleavage caused by the TFO. Here, depletion of the duplex target shifts the equilibrium toward triplex formation since less of the duplex remains intact. Finally, comparisons between the hybrids showed cleavage efficiencies following the trend: TFO3AI > TFO4CII > TFO4BI (**Figure 4b** and **Figure S-39**) but sequence discrimination was found to be significantly higher for TFOs bearing base modifications (*i.e*. Mod B & C). DNA damage is also dependent on the type and position of the alkyne modification with increased discrimination by TFO4CII suggesting the internal position contributes to lower *off*-target cleavage effects.

Detailed analysis of AMN activity by qPCR

Our next aim was to quantitatively determine the cleavage efficiency of the hybrid materials on a section of the GFP gene containing the appropriate triplex recognition site. An assay was designed using real-time polymerase chain reaction (qPCR) to assess how TFO recognition and ultimately targeted oxidative DNA cleavage impacts the PCR cycle (**Figure 5a & b**). During qPCR, a DNA polymerase, custom primers and a fluorescent reporter molecule are used to exponentially amplify a DNA sequence of interest. Successful amplification is monitored—in real time as the reaction progresses—by detecting the fluorescent signal after every PCR cycle, which correlates to the concentration of double-stranded DNA present. Internally modified TFO4C hybridised to $6N_3$-TPMA (I) and $5N_3$-TPMA (II) ligands were selected for this study as they displayed high sequence discrimination during the earlier gel electrophoretic analysis (**Figure 4**).

Firstly, the DNA target sequence—a 113 bp section of the GFP gene containing the recognition sequence for TFO4—was amplified by *Taq* DNA polymerase and the relative concentration of DNA was monitored through SYBR green fluorescence. The initial concentration of intact duplex DNA is directly proportional to the number of PCR cycles required to achieve a fluorescent signal (threshold cycle, C_T). The qPCR assay was then carried out in the presence of non-clicked Cu-TPMA, the alkyne-TFO and increasing concentrations of Na-*L*-asc. In this instance, no significant DNA damage was observed until 250 equivalents of reductant were present in the reaction mixture (**Figure 5c** (Cu-TPMA)**;** fold change at 250 eq. Na-*L*-asc = 0.58). When Cu(II)-bound AMN-TFO hybrids were introduced to the qPCR mixture in the absence of exogenous reductant, DNA cleavage was immediately identified as the amplification efficiency was significantly impeded and a fold change of 0.54 was obtained for both TFO4CI and TFO4CII (**Figure 5c** (Cu-TFO4CI & Cu-TFOCII)). While in the presence of increasing concentrations of ascorbate—a reductant natively present in biological systems—the target duplex was ablated by both AMN-TFO hybrids (fold change at 1000 eq. Na-*L*-asc = ~0.10). TFO4CI and TFO4CII display similar cleavage profiles, while attenuated cleavage by the non-clicked Cu(II)-TPMA complex with alkyne-TFO was observed. Overall, this result indicates instantaneous sequence recognition and hybridisation of the Cu(II)-bound AMN-TFO hybrids to the DNA target sequence followed by site specific cleavage.

Mechanistic studies on the plasmid GFP cloning vector

We analysed the cleavage effects of TFO4CII using a closed circular pCSanDI-HYG plasmid (6389 bp) containing the target sequence. The AMN-hybrid in the presence of 50 equivalents of Na-*L*-asc converted supercoiled (SC) plasmid to the nicked open circular (OC) form with the linear (L) form—indicative of a double strand break—arising at 100 equivalents and above (**Figure 6a**). To probe the radical species involved in the cleavage pathway,

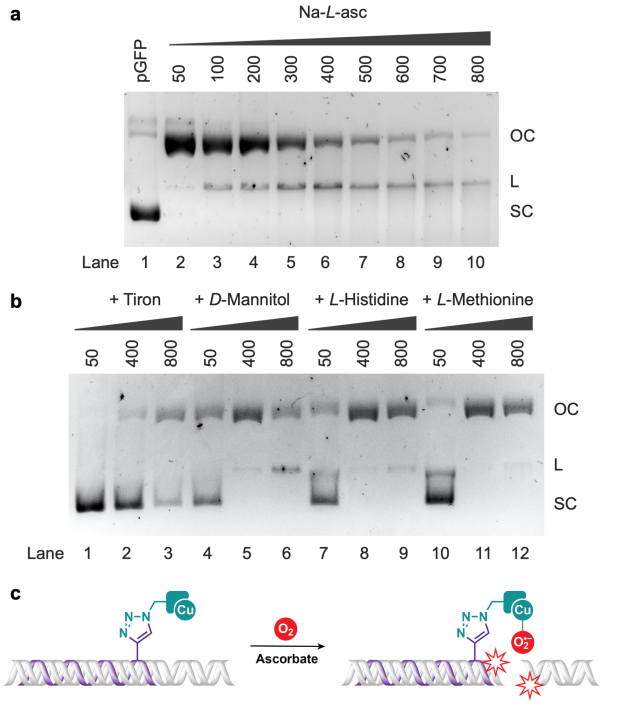

Figure 6. a Catalytic nuclease activity of TFO4CII on pGFP supercoiled DNA; pGFP (200 ng) treated with 250 eq of TFO4CII in the presence of increasing concentrations of Na-*L*-asc (50-800 eq to TFO4CII, lanes 2-10); **b** pGFP (200 ng) treated with 250 eq of TFO4CII with increasing Na-*L*-asc (50-800 eq, corresponding to lanes 2, 6, and 10 in A) in the presence of 10 mM scavenging species 4,5-dihydroxy-1,3-benzenedisulfonic acid (tiron, lanes 1-3), *D*-mannitol (lanes 4-6), *L*-histidine (lanes 7-9) and *L*-methionine (lanes 10-12); **c** Simplified mechanism for the generation of the superoxide radical by the AMN-TFO hybrid.

experiments were performed with ROS scavengers: tiron (superoxide, $O_2^{\bullet-}$); *D*-mannitol (hydroxyl radical, $^{\bullet}OH$); *L*-histidine (singlet oxygen, $^1O_2$); and *L*-methionine (H_2O_2, $^{\bullet}OH$, and HOCl). It is clear that AMN-hybrids excise DNA primarily through superoxide radical production (presumably as Cu(II)-$O_2^{\bullet-}$ adducts)[41] as preincubation with tiron impedes damage of SC-DNA, which delays the onset of nicking and inhibits double strand damage (**Figure 6b**, lanes 1-3). Other radical species are involved to a lesser extent and follow an inhibition profile of H_2O_2 > $^1O_2$ > $^{\bullet}OH$. Significantly, these results agree with previous findings where free Cu-TPMA and several other Cu-TPMA-Phenanthrene derivatives damage pUC19 plasmid DNA primarily through a superoxide radical-mediated pathway (**Figure 6c**).[14] The similarity between the free complexes and AMN hybrids suggest the ON vector does not alter the radical oxidation chemistry promoted by the metal complex.

Application of strain-promoted and thiazole orange substituents

To expand the scope of this technology, attempts to develop AMN-TFOs using bio-orthogonal chemistry—a selective reaction possible in living systems without interference to the native biochemical process—were investigated. One type of bio-orthogonal reaction is strain-promoted azide-alkyne cycloaddition (SPAAC) which operates *in-situ* without the need for copper catalysis.[49] We functionalised TFO4 with a 5′-phosphate-BCN (bicyclo[6.1.0]nonyne; **Mod D**) and successfully coupled the azide-modified ligands I-III *via* SPAAC (**Figure 7a**). Similar to CuAAC hybrids, AMN ligands clicked to TFO4D displayed lower T_M values with the introduction of 1 equivalent of Cu(II) affording additional triplex stability. To develop the AMN-TFO probes even further, the introduction of an intercalator that can overcome triplex instability was explored.[48] TFO4D was modified with a 5-(1-propargylamino)-2′-deoxyuridine (pdU) internally (i-TOTFO)

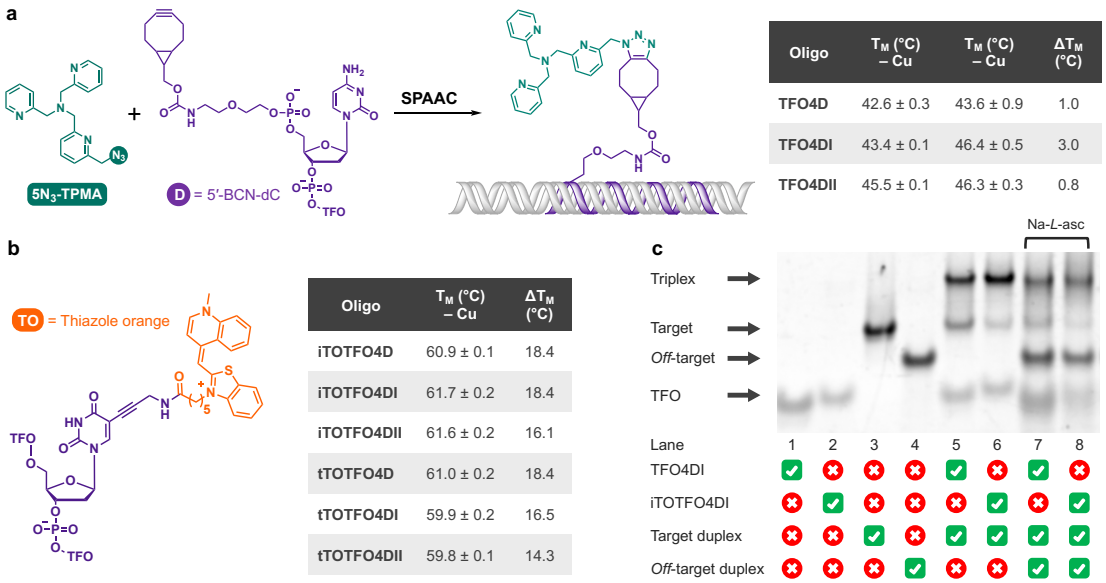

Oligo	T_M (°C) – Cu	T_M (°C) – Cu	ΔT_M (°C)
TFO4D	42.6 ± 0.3	43.6 ± 0.9	1.0
TFO4DI	43.4 ± 0.1	46.4 ± 0.5	3.0
TFO4DII	45.5 ± 0.1	46.3 ± 0.3	0.8

Oligo	T_M (°C) – Cu	ΔT_M (°C)
iTOTFO4D	60.9 ± 0.1	18.4
iTOTFO4DI	61.7 ± 0.2	18.4
iTOTFO4DII	61.6 ± 0.2	16.1
tTOTFO4D	61.0 ± 0.2	18.4
tTOTFO4DI	59.9 ± 0.2	16.5
tTOTFO4DII	59.8 ± 0.1	14.3

Figure 7. a Generation of AMN hybrid TFO4DI using SPAAC. **b** Structure of pdU modification with thiazole orange dye conjugated to the TFO (left), T_M of TOTFOs; t = TO attached towards 3'-end of TFO, i = internally attached TO, ΔT_M = change in T_M between TFO4D and TO-TFOD4. **c** GFP target and *off*-target (1.25 pmol) treated with a 25 eq of copper(II) bound hybrids TFO4DI and i-TOTFO4DI in the presence of 1000 eq of Na-*L*-asc (lane 7 and 8).

and towards the 3′-end (t-TOTFO) to allow NHS ester labelling of the TFO with thiazole orange (TO), an intercalating fluorophore known to increase the stability of triplexes. The introduction of TO greatly enhances the stability of TO-TFO4D (+18.4 °C) and this stability remains when the AMN ligands are clicked (**Figure 7b**). With enhanced stability, AMN-TOTFOs maintain their cleavage capability suggesting TO intercalation does not affect strand scission (**Figure 7c**). Comparison of the triplex band in lane 5 and 6 show stronger binding effects of TO-TFO4D compared to TFO4D. It is also evident from the depletion of this band in lane 8 compared to lane 6 that efficient cleavage is occurring with minimal *off*-target cleavage effects.

Conclusions

We applied nucleic acid click chemistry to engineer a new class of chemistry-based targeted nucleases whereby a metal-based cutting unit was directly coordinated to a guiding oligonucleotide (ON). The approach addresses existing limitations in the preparation of metal complex-ON hybrids, the low stability associated with metal ion dissociation, along with poor target selectivity and the dependence of an adjuvant (*e.g.* spermine) to stabilize DNA triplexes. Triplex forming oligonucleotides (TFOs) represent a strategic choice since Hoogsteen base pairing makes them easily programmable to target extended sequences that do not disrupt dsDNA structure during the recognition process. Two components were principally employed here: *i.*) a parallel triplex forming oligonucleotide (TFO) that binds sequence specifically to a gene fragment, and *ii.*) a copper binding artificial metallo-nuclease (AMN) that was conjugated *via* nucleic acid click chemistry to the TFO probe strand. The use of click chemistry provides a facile method to prepare library combinations that vary in probe length (16-32 nt), modification placement, and copper-binding scaffold. The scaffolds developed were azide-modified $5N_3$-TPMA and $6N_3$-TPMA (TPMA = *tris*-(2-picolyl)amine) that contain 'caging' chelators that bind, and stabilise, copper(II) ions using four nitrogen donors. The use of polypyridyl ligands represents a new approach compared to existing hybrids systems where Cu-Phen intercalators with limited solution stability have been employed.[24,26] By exploiting the unique base-triplet recognition properties of TFOs, purine-rich tracts of the green fluorescent protein (GFP) gene were efficiently targeted and cleaved by copper-bound hybrids. Visualisation of triplexes by polyacrylamide gel electrophoresis identified cleavage responses consistent with oxidative damage. Quantitative PCR analysis identified target cleavage in the absence of added reductant, while complete ablation was achieved in the presence of added reductant. The hybrids cleaved circularly closed GFP plasmid DNA (6389 bp) and their oxidative cutting mechanism relies (primarily) on the generation of superoxide type radicals. To extend the boundaries of this technology, hybrid systems were engineered using bio-orthogonal methods using strain-promoted substituents with thiazole orange modifications that augment triplex stability. Using this approach, stabilisation toward the melting of DNA triplexes increased by up to +18 °C. Further refinements of this class may involve the introduction of multiple TO modifications to enable triplex stabilization at neutral pH—an effect recently observed by Walsh *et al*.[48] Importantly, cleavage in absence of reductant and the stabilization afforded by thiazole orange modifications distinguish this technology from existing AMN-TFOs where polycationic species and exogenous reductants are required to achieve appropriate triplex formation and cleavage.[24,26] Further refinements to progress these hybrids towards cellular applications may include the development of AMNs that provide enhanced DNA cleavage, with catalytic cores that limit diffusible radical production which will reduce undesirable *off*-target cleavage effects. Exploiting synthetic triplex motifs with backbone and ribose modifications may offer improved resistance to free radical oxidation and provide enhanced cellular targeting properties to this type of chemistry-based hybrid gene targeted system. In this regard, future *in vivo* studies involving these hybrid systems could employ modifications such as phosphorthioate backbones, 2'-*O*-methyl, or inverted dT functionalities to increase cellular uptake and enhance stability towards endo- and exo-nucleases.

Experimental Section

MATERIALS AND METHODS

Chemicals, reagents and high-performance liquid chromatography (HPLC) grade solvents including $CHCl_3$, MeOH and CH_3CN were purchased from Merck (Ireland) or Tokyo Chemical Industry (TCI, UK Ltd) and used without further purification. ^1H, ^{13}C NMR and 2D-NMR (^1H-^1H COSY and ^1H-^{13}C HSQC) spectra were obtained on a Bruker AC 600 MHz NMR spectrometer (C-1). pH was monitored using a Mettler Toledo InLab Expert Pro-ISM pH probe. Electrospray ionization mass spectrometry (ESI-MS) measurements were recorded on a Bruker HCT-MS with samples prepared in 100% HPLC-grade CH_3CN prior to ESI-MS analysis. UV/Vis absorption spectroscopy studies were carried out on a Shimadzu UV-2600 spectrophotometer. FTIR measurements were conducted on a PerkinElmer Spectrum Two spectrometer. Thermal melting analysis was carried out on an Agilent Cary 100 dual beam spectrophotometer equipped with a 6 × 6 Peltier multicell system and temperature controller or an Agilent Cary 4000 UV-Visible spectrophotometer from Varian. PAGE and agarose gels were photographed using a Syngene G:Box mini 9 imaging system. Real-time PCR (qPCR) analysis was performed on a Roche LightCycler® 480 II using SYBR Green I Master mix (Roche). X-ray diffraction data were collected at 100(2)K on a Synergy, Dualflex, AtlasS2 diffractometer using CuKα radiation. The structure was solved by dual space methods and refined on F^2 using all the reflections (SHELXL-2018).

Route A: Synthesis of *N*-5-(azidomethyl)pyridine-*N*-*di*-(2-picolyl)amine ($5N_3$-TPMA)

2,5-Pyridine dicarboxylic acid dimethyl ester (1a)

1a was synthesized according to a procedure previously reported by Kramer *et al*.[50] A suspension of 2,5-pyridinedicarboxylic acid (20.011 g, 119.74 mmol) in MeOH (55 mL) and conc. H_2SO_4 (4.5 mL) was refluxed overnight, neutralized with a saturated aqueous solution of $NaHCO_3$, and extracted with $CHCl_3$ (3 × 150 mL). The

combined organic phases were dried over $MgSO_4$ and the solvent removed *in vacuo* to yield the diester product **1a** as a white solid (16.712 g, yield = 71.5%). ^{1}H-NMR (600 MHz, $CDCl_3$): δ 9.24 (dd, J = 2.1, 0.7 Hz, 1H), 8.39 (dd, J = 8.1, 2.1 Hz, 1H), 8.15 (dd, J = 8.1, 0.7 Hz, 1H), 3.98 (s, 3H), 3.93 (s, 3H). ^{13}C-NMR (151 MHz, $CDCl_3$): δ 164.9, 164.8, 150.8, 150.7, 138.3, 128.6, 124.7, 53.2, 52.7.

2,5-Bis(hydroxymethyl)pyridine (2a)

2a was synthesized according to a procedure previously reported by Kramer *et al*.[50] $NaBH_4$ (0.390 g, 10.30 mmol) was added slowly to a suspension of **1a** (0.502 g, 2.57 mmol) in EtOH (10 mL) at 0 °C. The solution was stirred for 1 h at 0 °C, then for 3 h at room temperature, and finally at reflux overnight. The solvent was removed and the resulting yellow oil was dissolved in a mixture of acetone (50 mL) and saturated aqueous solution of K_2CO_3 (50 mL), refluxed for 1 h and the yellow organic phase collected from a bi-phasic mixture. The solvent was removed and the crude product purified *via* dry column vacuum chromatography (DCVC silica gel, CH_2Cl_2:MeOH, 7:1 v/v) to yield the diol **2a** as a yellow, hygroscopic oil (0.204 g, yield = 57.0%). ^{1}H-NMR (600 MHz, MeOD-d_4): δ 8.46 (d, J = 1.6 Hz, 1H), 7.84 (dd, J = 8.0, 2.0 Hz, 1H), 7.54 (d, J = 8.0 Hz, 1H), 4.70 (s, 2H), 4.65 (s, 2H). ^{13}C-NMR (151 MHz, MeOD): δ 161.2, 148.1, 137.6, 137.3, 121.8, 65.4, 62.4.

2-Formyl-5-hydroxymethylpyridine (3a)

3a was synthesized according to a procedure reported by Dawson *et al*.[51] Under inert atmosphere, **2a** (8.277 g, 59.49 mmol) was dissolved in 1,4-dioxane (80 mL) and H_2O (2 mL) and SeO_2 (3.386 g, 30.51 mmol) was added. The mixture was degassed and heated under argon at 100 °C for 3 h. The solution was then filtered through a celite pad (30 mL dioxane wash), reduced in volume to ~ 5 mL, and purified *via* DCVC (silica gel, hexane:ethylacetate, gradient 50:50 to 25:75 v/v). The fractions of the product were combined, and solvent removed *in vacuo* to yield **3a** as a pale yellow solid (6.633 g, yield = 81.3%). ^{1}H-NMR (600 MHz, $CDCl_3$): δ 10.1 (d, J = 0.8 Hz, 1H), 8.77 (dd, J = 2.0, 0.7 Hz, 1H), 7.97 (dd, J = 8.0, 0.7 Hz, 1H), 7.90 (dq, J = 8.0, 2.1, 0.8 Hz, 1H), 4.87 (s, 2H, CH_2). ^{13}C-NMR (151 MHz, $CDCl_3$): δ 193.2, 152.4, 148.8, 140.9, 135.4, 121.8, 62.5.

5-Hydroxomethyl-*di*-(2-pycolyl)amine (4a)

To a solution of 2-picolylamine (0.179 g, 1.65 mmol) in MeOH (20 mL), a solution of **3a** (0.229 g, 1.67 mmol) in MeOH (20 mL) was added at 0 °C, stirred for 1 h at room temperature and $NaBH_4$ (0.063 g, 1.66 mmol) was added at 0 °C. The reaction was stirred at room temperature overnight. A minimal volume of H_2O was added and MeOH was removed *in vacuo*. The solution was acidified with conc. HCl to pH ~ 4 and extracted with CH_2Cl_2 (6 x 20 mL). $NaHCO_3$ was slowly added to the aqueous layer to reach pH ~ 8, extracted with CH_2Cl_2 (3 x 100 mL) and the combined organic layers were dried over $MgSO_4$. The solvent was removed to afford **4a** as a yellow oil (0.170 g, yield = 44.9%). ^{1}H-NMR (600 MHz, $CDCl_3$): δ 8.56 (dq, J = 4.9, 1.5, 0.8 Hz, 1H), 8.53 (d, J = 1.8 Hz, 1H), 7.67 (dd, J = 8.0, 2.2 Hz, 1H), 7.64 (td, J = 7.6, 1.8 Hz, 1H), 7.37 (d, J = 7.9, Hz, 1H), 7.35 (d, J = 7.9 Hz, 1H), 7.16 (qd, J = 7.4, 4.9, 0.9 Hz, 1H), 4.71 (s, 2H), 3.99 (s, 2H), 3.97 (s, 2H). ^{13}C-NMR (151 MHz, $CDCl_3$): δ 195.8, 149.4, 148.3, 136.6, 135.6, 122.4, 122.3, 122.2, 63.0, 54.8, 54.62.

5-Hydroxomethyl-*tris*-(2-pycolyl)amine (5a)

4a (0.130 g, 0.57 mmol) was dissolved in CH_3CN (15 mL) and stirred with $NaHCO_3$ (0.097 g, 1.15 mmol). 2-pycolylchloride (0.072 g, 0.57 mmol) in CH_3CN (15 mL) was added dropwise and the mixture was stirred at 50 °C for 72 h. The solution was filtered and the filtrate evaporated to afford **5a** as a brown oil. (0.135 g, yield = 74.4%) ^{1}H-NMR (600 MHz, $CDCl_3$): δ 8.51 (dq, J = 4.8, 1.6, 0.8 Hz, 2H), 8.47 (d, J = 1.7 Hz, 1H), 7.69 (dd, J = 8.0, 2.2 Hz, 1H), 7.64 (td, J = 7.7, 1.8 Hz, 2H), 7.57 (d, J = 2.7 Hz, 2 H), 7.55 (d, J = 2.9 Hz, 1 H), 7.13 (qd, J = 7.4, 4.9, 1.1 Hz, 2H), 4.68 (s, 2H), 3.85 (s + s, 6H).

5-Chloromethyl-*tris*-(2-pycolyl)amine (6a)

A modification of the literature procedure by Sprakel *et al.* was employed.[52] A solution of **5a** (0.396 g, 1.24 mmol) in $CHCl_3$ (5 mL) was added dropwise at 0 °C to a solution of $SOCl_2$ (0.450 mL, 6.18 mmol) in $CHCl_3$ (10 mL) and stirred overnight at room temperature. The solvent was removed *in vacuo* and the green product was dissolved in THF (5 mL) and DIPEA (0.808 mL) and stirred under argon for 3 h at room temperature and filtered through a celite pad (25 mL THF wash). Solvent was removed *in vacuo* to yield **6a** as a brown solid. (0.381 g, yield = 90.9%) ^{1}H NMR (600 MHz, $CDCl_3$): δ 8.54 (dq, J = 4.8, 1.8, 0.9 Hz, 2H), 8.52 (d, J = 1.9 Hz, 2H), 7.69 (dd, J = 8.1, 2.3 Hz, 1H), 7.65 (td, J = 7.7, 1.8 Hz, 2H), 7.60 (d, J = 8.1 Hz, 1 H), 7.56 (d, J = 7.8 Hz, 2 H), 7.14 (qd, J = 7.4, 4.9, 1.2 Hz, 2H), 4.56 (s, 2H), 3.89 (s, 2H), 3.88 (s, 4H).

5-Azidomethyl-*tris*-(2-pycolyl)amine (7a)

To a solution of **6a** (0.381 g, 1.12 mmol) in CH_3CN (20 mL), NaN_3 (0.219 g, 3.37 mmol) was added. The mixture was stirred in the dark at 50 °C overnight, filtered through a celite pad and solvent removed. The product was dissolved in $CHCl_3$ (20 mL) and washed with H_2O (3 x 10 mL). The organic phase was dried to yield **7a** as a brown solid (0.148 g, yield = 38.3%) ^{1}H NMR (600 MHz, $CDCl_3$): δ 8.54 (dq, J = 7.2, 2.3, 1.2 Hz, 2H), 8.47 (s, 1H), 7.66 (td, J = 11.5, 2.7 Hz, 4H), 7.63 (d, J = 2.8 Hz, 4H), 7.56 (d, J = 11.6 Hz, 2 H), 7.15 (qd, J = 11.1, 7.4, 1.7 Hz, 2H), 4.35 (s, 2H), 3.90 (s, 2H), 3.89 (s, 4H).

Route B: Synthesis of *N*-6-(azidomethyl)pyridine-*N*-*di*-(2-picolyl)amine (6N_3-TPMA)

Synthesis of *di*-(2-picolyl)amine (DPA)

Di-(2-picolyl)amine was synthesized according to a procedure reported by Hamann *et al*.[53] To a solution of 2-picolylamine (2.011 g, 18.6 mmol) in MeOH (10 mL), a solution of 2-pyridinecarboxaldehyde (2.025 g, 18.9 mmol) in MeOH (10 mL) was added dropwise at 0 °C. The solution was stirred for 1 h at room temperature, $NaBH_4$ (0.704 g, 18.6 mmol) was added slowly at 0 °C and stirred at room temperature overnight. A minimal volume of water was added and MeOH was removed *in vacuo.* The solution was acidified with conc. HCl to pH ~ 4 and extracted with CH_2Cl_2 (6 x 20 mL). Na_2CO_3 was added slowly to the

aqueous layer until a pH ~ 10 was reached. The product was extracted with CH_2Cl_2 (3 x 25 mL) and the combined organic layers dried over $MgSO_4$. Solvent was removed *in vacuo* to yield DPA as a yellow oil. (1.761 g, yield= 47.5%). ^{1}H-NMR (600 MHz, $CDCl_3$): δ 8.55 (dq, J = 4.9, 1.9, 1.0 Hz, 1H), 7.64 (td, J = 7.7, 1.9 Hz, 1H), 7.35 (d, J = 7.8 Hz, 1H), 7.15 (qd, J = 7.5, 4.8, 1.2 Hz, 1H), 3.98 (s, 2H). ^{13}C-NMR (151 MHz, $CDCl_3$): δ 159.6, 149.2, 136.3, 122.2, 121.8, 54.7. ESI-MS: *m/z* calcd 200.1 $[M + H]^+$; found 200.1.

***N*-6-(chloromethyl)pyridine-*N*-*di*-(2-picolyl)amine (1b)**

1b was prepared according to the method reported by Pope *et al.* with slight modification.[54] To a solution of 2,6-*bis*(chloromethyl)pyridine (0.505 g, 2.86 mmol) in CH_3CN (15 mL), $NaHCO_3$ (0.241 g, 2.87 mmol) was added, followed by 1 eq. of *di*-(2-picolyl)amine (0.571 g, 2.86 mmol) in CH_3CN (15 mL). The mixture was stirred at 50 °C overnight and monitored by ^{1}H-NMR. The solution was filtered and the filtrate evaporated to dryness. The orange, oily residue was purified by column chromatography (silica gel, CH_2Cl_2:MeOH, 95:5 v/v). Fractions of **1b** were combined and the solvent removed to afford a yellow solid (0.349 g, yield = 36.0%). ^{1}H-NMR (600 MHz, $CDCl_3$): δ 8.53 (dq, J = 4.8, 1.7, 0.9 Hz, 2H), 7.68 (t, J = 7.7 Hz, 1H), 7.65 (td, J = 7.7, 1.8 Hz, 1H), 7.57 (d, J = 7.8 Hz, 2H), 7.54 (d, J = 7.7 Hz, 1H), 7.32 (d, J = 7.6 Hz, 1H), 7.14 (qd, J = 7.4, 4.9, 1.1 Hz, 2H), 4.64 (s, 2H), 3.90 (s, 4H), 3.89 (s, 2H). ^{13}C-NMR (151 MHz, $CDCl_3$): δ 159.4, 156.0, 149.2, 137.6, 136.6, 123.1, 122.3, 122.1, 121.1, 60.3, 60.0, 47.0. ESI-MS: *m/z* calcd: 361.1 $[M+H]^+$; found: 361.1.

***N*-6-(azidomethyl)pyridine-*N*-*di*-(2-picolyl)amine (2b)**

To a solution of **1b** (0.349 g, 1.03 mmol) in CH_3CN (15 mL), NaN_3 (0.214 g, 3.29 mmol) was added, stirred in the dark at 50 °C overnight, filtered over a celite pad and evaporated to dryness. The product was dissolved in $CHCl_3$ (20 mL) and washed with H_2O (3 x 10 mL). The organic phase was dried to yield **2b** as a brown solid (0.097 g, yield = 27.4%). ^{1}H-NMR (600 MHz, $CDCl_3$): δ 8.53 (d, J = 4.4 Hz, 2H), 7.68 (t, J = 7.7 Hz, 1H), 7.65 (td, J = 7.6, 1.8 Hz, 2H), 7.58 (d, J = 7.7 Hz, 2H), 7.54 (d, J = 7.7 Hz, 1H), 7.18 (d, J = 7.6 Hz, 1H), 7.14 (q, J = 6.3, 5.0 Hz, 2H), 4.44 (s, 2H, CH_2), 3.88 (d, 6H, CH_2). ^{13}C-NMR (151 MHz, $CDCl_3$): δ 159.8, 159.5, 155.2, 149.3, 137.5, 136.6, 123.1, 122.3, 122.2, 120.3, 60.4, 60.1, 55.8. ESI-MS: *m/z* calcd: 368.2 $[M+Na]^+$; found: 368.2.

Crystal Data. for $[Cu(6N_3\text{-TPMA})(NO_3)](NO_3)\cdot\frac{1}{2}CH_3CN$: $C_{20}H_{20.5}N_{9.5}O_6Cu$ (*M* =553.50 g/mol): triclinic, space group $P\bar{1}$ (no. 2), *a* = 10.6029(2) Å, *b* = 14.9442(4) Å, *c* = 15.8857(4) Å, *α* = 68.947(2)°, *β* = 82.439(2)°, *γ* = 82.246(2)°, *V* = 2318.19(11) Å^3, *Z* = 4, *T* = 100.00(10) K, μ(CuKα) = 1.855 mm^{-1}, D_{calc} = 1.586 g/cm^3, 21435 reflections measured (8.45° ≤ 2θ ≤ 153.396°), 9502 unique (R_{int} = 0.0269, R_{sigma} = 0.0350) which were used in all calculations. The final *R*1 was 0.0350 (I > 2σ(I)) and *wR*2 was 0.0914 (all data). Supplementary crystallographic data for this paper (CCDC 1939154) can be obtained free of charge from The Cambridge Crystallographic Data Centre *via* www.ccdc.cam.ac.uk/data_request/cif.

Click reactions

Oligonucleotide synthesis and purification

Alkyne-modified TFOs and dsDNA targets were synthesised by solid phase synthesis using an automated DNA synthesiser (Applied Biosystems 394) according to standard methods. Coupling efficiencies were monitored by the trityl cation conductivity monitoring facility and were greater than 98% for all oligonucleotides (ODNs). Modified phosphoramidites such as Mod A, B and C were purchased from Glen Research and Mod D from Berry and Associates. 5-(1-propargylamino)-dU phosphoramidite as well as thiazole orange was synthesised according to previously determined conditions.[48] ODNs were deprotected and cleaved in standard aqueous ammonia by heating for 5 h at 55 °C and were purified by gradient reverse phase HPLC (C8 size exclusion column) in 0.1 M Triethylammonium acetate (TEAA) buffer with 50% CH_3CN. Gradients of 10-40% over 20 minutes were used with 4 mL/min flow rate before desalting using NAP-25 (GE Healthcare). Purity of TFOs and dsDNA were analysed by ESI-MS (C-3). TFOs containing pdU were labelled with TO following a procedure by Walsh *et al.*[48]

CuAAC 'click' reaction of TFOs with AMN-ligands

The CuAAC reactions were performed according to the Lumiprobe protocol for click-chemistry labeling of oligonucleotides with minor modifications. In a final volume of 3 mL (50:50, H_2O:DMSO), 60 nmols of the alkyne-modified TFOs, 90 nmols of azide-modified ligand ($6N_3$-TPMA, $5N_3$-TPMA or $4N_3$-Benzyl-DPA) and 1.5 μmols of Na-*L*-asc were added. Reaction mixtures were degassed with nitrogen and 1.5 μmol of Cu-TBTA complex in DMSO (55% aqueous solution) was added. Solutions were further degassed, stirred overnight, quenched with 30 μmol of EDTA and desalted using NAP-25 columns. The volume was reduced and clicked TFOs were purified by gradient (0.1 M NH_4OAc + 50% CH_3CN in NH_4OAc) reverse phase HPLC (C8 size exclusion column) to yield the final products (33-67%). Purity of the AMN-TFOs were determined by ESI-MS (Appendix C-3 and C-4).

Triplex formation studies

Thermal melting of the TFO triplexes in absence and presence of Cu(II). Solutions for thermal melting analysis containing 5 μM TFO and 2 μM target duplex (2.5:1 TFO:duplex) were prepared in a final volume of 100 μL buffer (10 mM PO_4^{3-}, 150 mM NaCl, 2 mM $MgCl_2$, pH ~ 6). Prior to analysis, TFOs and target duplexes were denatured by heating to 90 °C (10 °C/min, 2 min hold) and reannealed at 12 °C (0.5 °C/min, 20 min hold). In experiments containing Cu(II), 5 μM $Cu(ClO_4)_2$ was added at this point (1:1 ratio with TFO). Thermal melting analysis was recorded at 260 nm using Starna black-walled quartz cuvettes with tight-fitting seals in the range of 12-90 °C (0.5 °C/min, 2 min hold). A total of three heating ramps were carried out and T_M calculated as an average of the first derivative of the sigmoidal regression fit of the triplex melting curve on Graphpad Prism® 6.0 software.

DNA damage studies
Stock solutions of AMN-TFOs and target duplexes were initially prepared in nuclease-free water and further dilutions prepared in reaction buffer (10 mM PO_4^{3-}, 150 mM NaCl, 2 mM $MgCl_2$, pH ~ 6). 1 *eq.* of Cu(II) ($Cu(ClO_4)_2$) was added to the AMN-TFO stock solutions and incubated for 15 minutes prior to further use.

Cleavage efficacy of AMN-TFO hybrids
In a total volume of 5 μL, a target DNA duplex sequence (52 bp, 1.25 pmol) was exposed to increasing eq. of TFO4CII in the presence of Na-*L*-asc (3.125 mM). Reaction mixtures were vortexed and incubated at 37 °C for 6 h, quenched with 6X loading dye and loaded onto a 20% polyacrylamide gel (50 mM Trizma, 5 mM $MgCl_2$, pH ~ 6). Electrophoresis was carried out at 70 V for 6 h in Trizma buffer (50 mM, pH ~ 6) and post-stained with SybrGold.

Catalytic activity of AMN-TFO hybrids
A target DNA duplex sequence (52 bp, 1.25 pmol) was exposed to TFO4CII (31.25 pmol) in the presence of increasing equivalents of Na-*L*-asc for 6 h at 37 °C with electrophoresis and staining carried out as previously stated.

qPCR analysis of catalytic activity
A 113 bp region of the pCSanDI-HYG plasmid (containing the target site for TFO4) was amplified by PCR (forward primer: 5'-AAAGGGAGCCCCCGATTTAG-3' and reverse primer: 5'-GTGACCGCTACACTTGCCA-3') and amplicons purified using Monarch® PCR & DNA clean-up kit (NEB, T1030). In a total volume of 12 μL, the target DNA duplex (113-mer, 1.25 pmol) was exposed to each hybrid material (31.25 pmol of either TFO4CI, TFO4CII or TFO4CIII) in the presence of increasing equivalents of Na-*L*-asc. Reaction mixtures were vortexed. At t = 0 h, 6 μL of the reaction volume was quenched with EDTA (90 nmol) and kept as a control. The remaining 6 μL was incubated at 37 °C for 6 h (target) prior to addition of EDTA. Control and target samples were diluted ($1:10^5$) and qPCR analysis was performed over 45 cycles (LightCyler 480 II). Each sample was prepared as per kit protocol using LightCycler 480 SYBR green I master kit (Roche, 04887352001). The change in threshold cycle (C_T) between the target (6 h) and control sample (0 h) (target C_T – control C_T) was calculated (ΔC_T). ΔC_T were plotted as linear values ($2^{-\Delta CT}$). The $2^{-\Delta CT}$ values were normalised to the untreated duplex yielding a $2^{-\Delta\Delta CT}$ plot.

Target and *off*-target cleavage discrimination. In a total volume of 5 μL, a mixture of target and *off*-target (no triplex recognition) DNA duplex sequences was exposed to 25 eq of each hybrid material (TFO3AI, TFO4AIII, TFO4BI, TFO4CII or a 1:1 mixture of free Cu-TPMA and TFO4C) in the presence of increasing equivalents of Na-*L*-asc for 6h at 37 °C. Electrophoresis and staining was carried out as previously stated.

pCSanDI-HYG cleavage efficacy. In a total volume of 5 μL, pCSanDI-HYG (200 ng, 0.05 pmol) was treated with 250 eq of TFO4CII in the presence of increasing concentrations of Na-*L*-asc (50-800 eq to TFO4CII) for 6 h at 37 °C. Reactions were quenched with 6X loading dye and loaded onto a 1% agarose gel containing 10 μL SYBR Safe and subjected to electrophoresis at 70 V for 3 h in TAE buffer (1X).

pCSanDI-HYG cleavage in the presence of ROS scavengers. In a total volume of 5 μL, pCSanDI-HYG (200 ng, 0.05 pmol) was treated with 250 eq of TFO4CII and increasing concentrations of Na-*L*-asc (50-800 eq to TFO4CII), in the presence of 10 mM scavenging species 4,5-dihydroxy-1,3-benzenedisulfonic acid (tiron), *D*-mannitol, *L*-histidine and *L*-methionine. Reactions were vortexed and incubated at 37 °C for 6 h. Agarose gel electrophoresis carried out as above.

Acknowledgements

AK and TB acknowledge funding from the Marie Skłodowska-Curie Innovative Training Network (ITN) ClickGene (H2020-MSCA-ITN-2014-642023). AK also acknowledges funding from Science Foundation Ireland Career Development Award (SFI-CDA) [15/CDA/3648]. BMcG acknowledges funding from the Irish Research Council [GOIPG/2018/1427]. This publication has emanated from research supported in part by a research grant from Science Foundation Ireland (SFI) and is co-funded under the European Regional Development Fund under Grant Number 12/RC/2275_P2. Mass spectrometry and UV analysis were carried out at the Nano Research Facility in Dublin City University which was funded under the Programme for Research in Third Level Institutions (PRTLI) Cycle 5. The PRTLI is co-funded through the European Regional Development Fund (ERDF), part of the European Union Structural Funds Programme 2011-2015. TB and AHES acknowledges funding from the UK BBSRC (grants BB/J001694/2 and BB/R008655/1). We are grateful to the Carlsberg Foundation (grant CF15-0675) for funding towards the X-ray diffractometer. NZF would like to thank Dr. Alan Costello of the NICB for donation of pCSanDI-HYG plasmid.
† Authors contributed equally to this work.

Present Addresses
‡Nicolò Zuin Fantoni − Chemistry Research Laboratory, University of Oxford, 12 Mansfield Road, Oxford OX1 3TA, United Kingdom.

Conflict of Interest

The authors declare no conflict of interest.

Keywords: chemical nuclease • click chemistry • triplex forming oligonucleotides • copper • DNA oxidation.

[1] B. L. Stoddard, A. Khvorova, D. R. Corey, W. S. Dynan, K. R. Fox, *Nucleic Acids Res.* **2018**, *46*, 1563–1564.
[2] X. Shen, D. R. Corey, *Nucleic Acids Res.* **2018**, *46*, 1584–1600.
[3] M. Faria, C. Giovannangeli, *J. Gene Med.* **2001**, *3*, 299–310.
[4] A. C. Komor, Y. B. Kim, M. S. Packer, J. A. Zuris, D. R. Liu, *Nature* **2016**, *533*, 420–424.
[5] H. A. Rees, D. R. Liu, *Nat. Rev. Gen.* **2018**, *19*, 770–788.

[6] T. C. Johnstone, K. Suntharalingam, S. J. Lippard, *Chem. Rev.* **2016**, *116*, 3436–3486.
[7] D. S. Sigman, A. Mazumder, D. M. Perrin, *Chem. Rev.* **1993**, *93*, 2295–2316.
[8] A. Kellett, Z. Molphy, C. Slator, V. McKee, N. P. Farrell, *Chem. Soc. Rev.* **2019**, *48*, 971–988.
[9] J. Cadet, J. R. Wagner, *Cold Spring Harb. Perspect. Biol.* **2013**, *5:a012559*, 1–18.
[10] C. Marzano, M. Pellei, F. Tisato, C. Santini, *Anticancer Agents Med. Chem.* **2009**, *9*, 185–211.
[11] B. C. Bales, T. Kodama, Y. N. Weledji, M. Pitié, B. Meunier, M. M. Greenberg, *Nucleic Acids Res.* **2005**, *33*, 5371–5379.
[12] K. J. Humphreys, K. D. Karlin, S. E. Rokita, *J. Am. Chem. Soc.* **2002**, *124*, 8055–8066.
[13] S. Thyagarajan, N. N. Murthy, A. A. Narducci Sarjeant, K. D. Karlin, S. E. Rokita, *J. Am. Chem. Soc.* **2006**, *128*, 7003–7008.
[14] N. Zuin Fantoni, Z. Molphy, C. Slator, G. Menounou, G. Toniolo, G. Mitrikas, V. McKee, C. Chatgilialoglu, A. Kellett, *Chem. Eur. J.* **2019**, *25*, 221–237.
[15] N. Z. Fantoni, Z. Molphy, S. O'Carroll, G. Menounou, G. Mitrikas, M. G. Krokidis, C. Chatgilialoglu, J. Colleran, A. Banasiak, M. Clynes, S. Roche, S. Kelly, V. McKee, A. Kellett, *Chem. Eur. J.* **2020** (accepted, 10.1002/chem.202001996).
[16] Z.-R. Li, J. Li, W. Cai, J. Y. H. Lai, S. M. K. McKinnie, W.-P. Zhang, B. S. Moore, W. Zhang, P.-Y. Qian, *Nat. Chem.* **2019**, *11*, 880–889.
[17] R. Larragy, J. Fitzgerald, A. Prisecaru, V. McKee, P. Leonard, A. Kellett, *Chem. Commun.* **2015**, *51*, 12908–12911.
[18] A. Kellett, Z. Molphy, V. McKee, C. Slator, in *Metal-Based Anticancer Agents* (Eds.: A. Casini, A. Vessières, S.M. Meier-Menches), **2019**, pp. 91–119.
[19] C. Slator, Z. Molphy, V. McKee, C. Long, T. Brown, A. Kellett, *Nucleic Acids Res.* **2018**, *46*, 2733–2750.
[20] M. Pitié, C. J. Burrows, B. Meunier, *Nucleic Acids Res.* **2000**, *28*, 4856–4864.
[21] D. S. Sigman, T. W. Bruice, A. Mazumder, C. L. Sutton, *Acc. Chem. Res.* **1993**, *26*, 98–104.
[22] J. Gallagher, C. B. Chen, C. Q. Pan, D. M. Perrin, Y.-M. Cho, D. S. Sigman, *Bioconjugate Chem.* **1996**, *7*, 413–420.
[23] P. B. Dervan, *Isr. J. Chem.* **2019**, *59*, 71–83.
[24] J. C. François, T. Saison-Behmoaras, M. Chassignol, N. T. Thuong, C. Helene, *J. Biol. Chem.* **1989**, *264*, 5891–5898.
[25] S. A. Kane, S. M. Hecht, J.-S. Sun, T. Garestier, C. Helene, *Biochemistry* **1995**, *34*, 16715–16724.
[26] A. Panattoni, A. H. El-Sagheer, T. Brown, A. Kellett, M. Hocek, *ChemBioChem* **2020**, *21*, 991–1000.
[27] T. Lauria, C. Slator, V. McKee, M. Müller, S. Stazzoni, A. L. Crisp, T. Carell, A. Kellett, *Chem. Eur. J. 10.1002/chem.202002860*.
[28] P. G. Shultz, J. S. Taylor, P. B. Dervan, *J. Am. Chem. Soc.* **1982**, *104*, 6861–6863.
[29] P. G. Schultz, P. B. Dervan, *Proc. Natl. Acad. Sci. U.S.A.* **1983**, *80*, 6834–6837.
[30] H. Moser, P. Dervan, *Science* **1987**, *238*, 645–650.
[31] S. A. Strobel, P. B. Dervan, *Science* **1990**, *249*, 73–75.
[32] Y. Aiba, J. Sumaoka, M. Komiyama, *Chem. Soc. Rev.* **2011**, *40*, 5657–5668.
[33] F. H. Zelder, A. A. Mokhir, R. Krämer, *Inorg. Chem.* **2003**, *42*, 8618–8620.
[34] G. Gasser, A. Pinto, S. Neumann, A. M. Sosniak, M. Seitz, K. Merz, R. Heumann, N. Metzler-Nolte, *Dalton Trans.* **2012**, *41*, 2304–2313.
[35] G. Gasser, K. Jäger, M. Zenker, R. Bergmann, J. Steinbach, H. Stephan, N. Metzler-Nolte, *J. Inorg. Biochem.* **2010**, *104*, 1133–1140.
[36] R. M. Cunningham, A. M. Hickey, J. W. Wilson, K. J. I. Plakos, V. J. DeRose, *J. Inorg. Biochem.* **2018**, *189*, 124–133.
[37] M. E. Núñez, K. T. Noyes, D. A. Gianolio, L. W. McLaughlin, J. K. Barton, *Biochemistry* **2000**, *39*, 6190–6199.
[38] G. B. Dreyer, P. B. Dervan, *Proc. Natl. Acad. Sci. U.S.A.* **1985**, *82*, 968–972.
[39] J. C. François, T. Saison-Behmoaras, C. Barbier, M. Chassignol, N. T. Thuong, C. Hélène, *Proc. Natl. Acad. Sci. U.S.A.* **1989**, *86*, 9702–9706.
[40] C. H. Chen, D. S. Sigman, *Proc. Natl. Acad. Sci. U.S.A.* **1986**, *83*, 7147–7151.
[41] B. C. Bales, M. Pitié, B. Meunier, M. M. Greenberg, *J. Am. Chem. Soc.* **2002**, *124*, 9062–9063.
[42] K. R. Fox, T. Brown, *Biochem. Soc. Trans.* **2011**, *39*, 629–634.
[43] K. R. Fox, T. Brown, D. A. Rusling, in *DNA-Targeting Molecules as Therapeutic Agents* (Ed.: M.J. Waring), Royal Society Of Chemistry, Cambridge, **2018**, pp. 1–32.
[44] E. Wang, S. Malek, J. Feigon, *Biochemistry* **1992**, *31*, 4838–4846.
[45] D. A. Rusling, V. E. C. Powers, R. T. Ranasinghe, Y. Wang, S. D. Osborne, T. Brown, K. R. Fox, *Nucleic Acids Res.* **2005**, *33*, 3025–3032.
[46] J. Gierlich, G. A. Burley, P. M. E. Gramlich, D. M. Hammond, T. Carell, *Org. Lett.* **2006**, *8*, 3639–3642.
[47] Z. Molphy, D. Montagner, S. S. Bhat, C. Slator, C. Long, A. Erxleben, A. Kellett, *Nucleic Acids Res.* **2018**, *46*, 9918–9931.
[48] S. Walsh, A. H. El-Sagheer, T. Brown, *Chem. Sci.* **2018**, *9*, 7681–7687.
[49] J. C. Jewett, C. R. Bertozzi, *Chem. Soc. Rev.* **2010**, *39*, 1272–1279.
[50] J. J. P. Kramer, M. Nieger, S. Bräse, *Eur. J. Org. Chem.* **2013**, *2013*, 541–549.
[51] M. I. Dawson, M. Park, R. L. S. Chan, D.Hobbs;N-Heterocyclic Retinoic Acid Analogues, Patent U.S. 4,526,787, July 2, **1985**.
[52] V. S. I. Sprakel, J. A. A. W. Elemans, M. C. Feiters, B. Lucchese, K. D. Karlin, R. J. M. Nolte, *Eur. J. Org. Chem.* **2006**, *10*, 2281–2295.
[53] J. N. Hamann, M. Rolff, F. Tuczek, *Dalton Trans.* **2015**, *44*, 3251–3258.
[54] S. J. A. Pope, R. H. Laye, *Dalton Trans.* **2006**, *25*, 3108–3113.

Entry for the Table of Contents

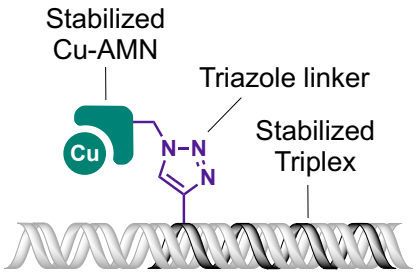

A click chemistry approach to targeted DNA oxidation is reported where azide-modified tripodal ligands are conjugated to alkyne-TFOs. In the presence of coordinated Cu(II) these hybrids efficiently target and cleave purine-rich genetic elements.

Institute and/or researcher Twitter usernames:
@andrew_kellett @NicoloFZuin @ZMolphy @B_McGorman @Prof_Tom_Brown
@DCUChemistry @OxfordChemistry @nicb_dcu @DCUResearchNano @ATDBio